AAS 15-588

EARTH-MARS TRANSFERS THROUGH MOON DISTANT RETROGRADE ORBIT

Davide Conte[*], Marilena Di Carlo[†], Koki Ho[‡], David B. Spencer[§], and Massimiliano Vasile[¶]

This paper focuses on trajectory design which is relevant for missions that would follow NASA's Asteroid Redirect Mission (ARM) to further explore and utilize asteroids and eventually human Mars exploration. Assuming that a refueling gas station is present at a given Lunar Distant Retrograde Orbit (DRO), we analyze ways of departing from the Earth to Mars via that DRO. Thus, the analysis and results presented in this paper add a new cis-lunar departure orbit for Earth-Mars missions. Porkchop plots depicting the required C_3 at launch, v_∞ at arrival, Time of Flight (TOF), and total ΔV for various DRO departure and Mars arrival dates are created and compared with results obtained for low ΔV LEO to Mars trajectories. The results show that low ΔV DRO to Mars transfers generally have lower ΔV and TOF than LEO to Mars maneuvers.

INTRODUCTION

A Lunar Distant Retrograde Orbit (DRO) is an orbit that exists due to third-body effects. Such trajectory is the solutions of the Circular Restricted Three Body Problem (CR3BP) of a system in which Earths and Moons gravitational attractions are considered. A DRO is possibly a very critical stepping stone, both implicitly and literally, for our ultimate goal: human Mars exploration.

Compared with the other past destinations such as a low-Earth orbit or the Moon, Mars is distant from the Earth and its journey will not be short. We have learned from our history of exploration the importance of logistical considerations for such expeditions. Part of the logistics considerations in space exploration includes the locations of on-orbit propellant depots, in-situ resource utilization (ISRU) plants, and other types of space infrastructure.[1] Multiple recent studies have shown the promising effectiveness of having a propellant depot on the way to or back from the destination.[2,3]

A DRO has recently been proposed to be one of the most suitable locations to locate those space infrastructure. This is due to its orbital stability and easiness of access in terms of gravity well.[4,5] For example, a propellant depot can be at a DRO so that a cargo mission can visit that depot to be refueled before heading to its destination. In addition, a space station can also be located at a

[*]Ph.D. Candidate, Department of Aerospace Engineering, The Pennsylvania State University, 229 Hammond Building, University Park, PA, 16802.

[†]Ph.D. Candidate, Department of Mechanical and Aerospace Engineering, University of Strathclyde, James Weir Building, Glasgow G1 1XJ, United Kingdom.

[‡]Ph.D., Aeronautics and Astronautics, Massachusetts Institute of Technology, Cambridge, MA, 02139.

[§]Professor, Department of Aerospace Engineering, The Pennsylvania State University, 229 Hammond Building, University Park, PA, 16802.

[¶]Professor, Department of Mechanical and Aerospace Engineering, University of Strathclyde, James Weir Building, Glasgow G1 1XJ, United Kingdom.

DRO, which can be used as a maintenance base or safety haven for any unexpected contingencies in cis-lunar system. Moreover, a DRO can be used for the assembly of large spacecraft. This idea is attractive because it requires only two travels through the Van-Allen Radiation Belts as opposed to other high-Earth orbit (HEO) departure architectures.[6] Furthermore, the recent Asteroid Redirect Mission (ARM) proposed to redirect the asteroid to a DRO and send human there to gain knowledge and experiences for future Mars exploration.[5] A success of this mission would lead to further applications of a DRO.

In order to realize the above scenarios, the efficient transit path from Earth to Mars via a DRO (or the other way around) will be critical. Therefore, this paper aims to consider the Earth - DRO and DRO - Mars transfers. It computes the ΔV and TOF and generates porkchop plots for a given synodic period.

The analysis of LEO to DRO and DRO to Mars trajectories was supported by the following assumptions:

- ΔV maneuvers are treated as impulsive maneuvers.
- Earth-Moon dynamics is modelled as the Circular Restricted Three Body Problem (CR3BP) using an Earth-Moon mean distance of 384,400 km.
- Patched conics are used for interplanetary orbital transfers.
- Secular perturbations of other planetary bodies are neglected.

DRO USED FOR MARS MISSIONS

In order to show the value of a DRO for Mars exploration, a simple numerical example is shown. The considered scenarios assume a cargo mission, which can be a habitat pre-deployment mission preceding human missions. A propellant depot is assumed to be located at a DRO, and we are interested in the value of having such a propellant depot. More precisely, we want to find how much we can save our initial mass in low-Earth orbit (IMLEO) by refilling the propellant tanks from the depot at a DRO. Note that the cases with a depot cannot be simply compared against those without a depot because the depot development and launch costs are not considered. Instead, the result would give an indication about how much cost we are willing to pay to develop and launch such a propellant depot.

With the representative ΔV and TOF resulted from later analysis, the following scenarios are considered for the Mars mission.

- Scenario 1. Direct to Mars: The vehicle directly departs from Earth to Mars
- Scenario 2. Oxygen Refill in a DRO: The vehicle departs from Earth to a DRO, refills its oxygen tank from a propellant depot in the DRO, and heads to Mars.
- Scenario 3. Hydrogen and Oxygen Refill in a DRO: The vehicle departs from Earth to a DRO, refills its hydrogen and oxygen tanks from a propellant depot in the DRO, and heads to Mars.

The computation is simply based on the rocket equation. The assumed parameters are shown in Table 1 and the results are shown in Table 2. The ΔV and TOF values assume the synodic

period 2035-2036. Chemical rockets with a specific impulse (I_{sp}) of 450 s is assumed as the vehicle propulsion system. The refill operation is assumed to take 10 days. To represent the IMLEO reduction, the gear ratio is shown, which is defined as the ratio of IMLEO to the landed mass on Mars. In addition, the number of launches is also shown assuming the equivalent payload as NASA Design Reference Architecture 5.0 cargo pre-deployment mission (40 mT on Martian surface[7]) and the launches by the 130 mT Space Launch System (SLS).

Table 1. Assumed parameters (LMO: Low-Mars Orbit)

From	To	ΔV [km/s]	TOF [days]
LEO	LMO	5.76	202
LEO	DRO	3.82	6
DRO	LMO	3.29	206

Table 2. ΔV and TOF for each case

Scenario	Gear Ratio	TOF [days]	SLS launches
1	13.09	202	5
2	10.56	222	4
3	8.43	222	3

The results show that stopping at the DRO gas station would provide the propellant necessary for part or all of the rest of the journey to Mars, which would effectively reduce the propellant and the size of the tank that need to be launched from Earth. Thus, a smaller number of launches or smaller rockets could be used for the same payload mass to be sent to Mars. In the above case, the number of launches can be reduced from five to three, which can save the launch cost and time significantly. (Note that the current schedule for SLS launch frequency is only once a year.)

An example scenario of utilization of propellant depot in a DRO and lunar ISRU for a Mars cargo mission is shown in Figure 1. The first launch is a crewed mission that delivers the ISRU plant to the lunar surface and the propellant depot to a DRO. During the ISRU operation period, the human crew maintains the ISRU plant and performs science missions at the same time on the lunar surface. After the ISRU propellant generation, the generated propellant is delivered to the propellant depot in the DRO, and the human crew returns to Earth. In the meantime, the Mars cargo is launched and assembled in LEO, stops in a DRO to get refilled, and heads to Mars to deliver the cargo (e.g. habitat pre-deployment for later crew missions). Note that in this scenario, the propellant depot is assumed to be refilled by ISRU, but there are other possibilities for the usage of propellant depots.[3] This scenario provides an example how DROs can be used for Mars exploration, which thus motivates this research to compute the astrodynamics around a DRO.

EARTH - MOON DRO TRANSFER

No closed form solution for the DRO in the CR3BP exists. A collection of positions and velocities for points along the orbit can however be obtained by implementing a shooting method. Initial guesses for the shooting method are available in literature.[8] In Figure 2 and Figure 3 a Lunar DRO of 61,500 km amplitude is represented in the rotating reference frame of the CR3BP and in the inertial reference frame centered at the Earth. In Figure 2 the x axis points to the Moon and the y axis is perpendicular to it and both lie in the Earth-Moon plane. In Figure 3 x and y lie on an inertial

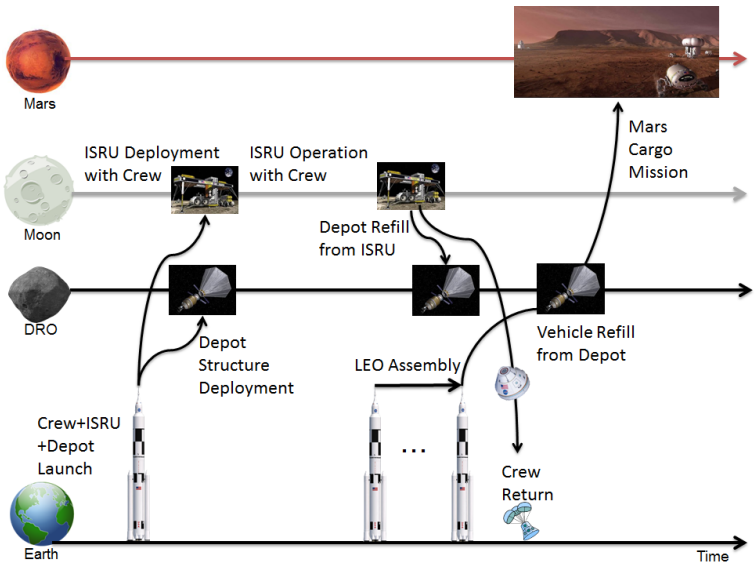

Figure 1. Bat chart for an example scenario of using DRO (Icon Credit: NASA, ULA)

plane centered at the Earth-Moon barycenter. An amplitude of 61,500 km was chosen for the DRO based on the work done at the Caltech Space Challenge 2015.[9]

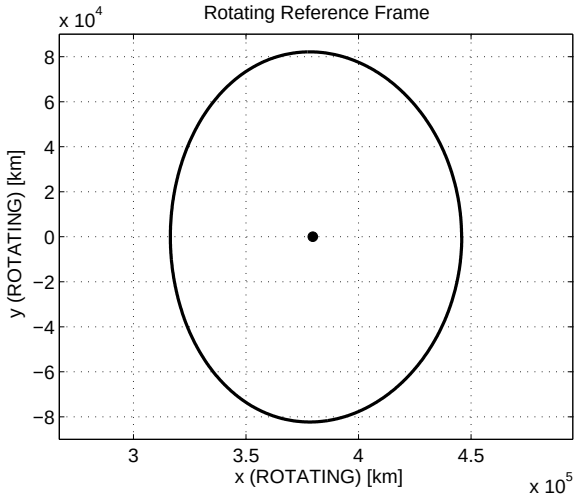

Figure 2. 61,500 km amplitude DRO in the rotating Earth-Moon reference frame

The orbit selection process for the transfer from Earth to Lunar DRO often comes to the trades between TOF and ΔV. Human missions typically prefer a trajectory with a short TOF even if the ΔV is not the minimum. This is due to crew health problems such as radiation dose limit and psychological problems. Chemical propulsion systems are often used for such missions. This trend is true for part of the robotic missions that requires a fast delivery as well. Most robotic missions, on the other hand, typically prefer a trajectory with a small ΔV even though their TOF is longer. For these missions, a low-thrust electric propulsion system, possibly with a low-energy transfer, is preferred to save the propellant.

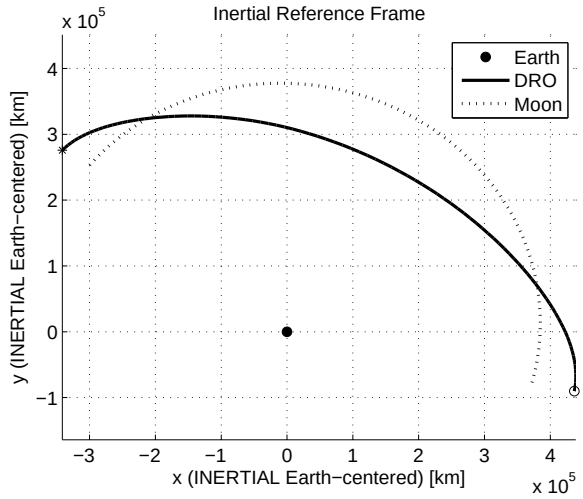

Figure 3. 61,500 km amplitude DRO in the inertial Earth-centered reference frame

For fast human missions, where a high thrust propulsion system (e.g. chemical) is preferred, the following transfer types have been considered:

- Direct transfer with lunar far side injection. This transfer requires two maneuvers, one to depart from LEO and one to insert into DRO,[10] with the injection occurring tangentially along the x axis of the Earth-Moon rotating reference frame. This transfer is shown in Figure 4.

- Prograde or retrograde powered lunar gravity assist. These transfers requires three maneuvers: departure from LEO, periselenium maneuver and injection maneuver, which can occur either with a prograde or retrograde motion. Retrograde transfers are typically less expensive in terms of injection ΔV.[8]

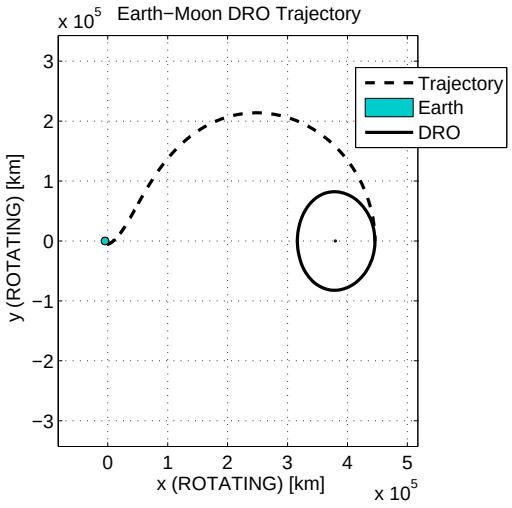

Figure 4. Direct Earth-DRO transfer

A direct transfer was chosen because of the reduced TOF and because the absence of Moon flyby maneuvers makes it safer for a human mission. The direct transfer from Earth to the DRO can be realized in 5.86 days; it requires a burnout velocity at the Earth of 10.91 km/s and a ΔV for the injection into the DRO of 619.82 m/s.

MOON DRO - MARS TRANSFER

In order to know the characteristic energy (C_3) the spacecraft needs to achieve to leave the Earth-Moon system and arrive at Mars at a certain arrival date, Earth-Mars porkchop plots were generated. The abscissa and ordinate on a porkchop plot represent the Earth-Moon departure and Mars arrival dates, respectively. The key parameters that are plotted on porkchop plots and used to investigate possible transfer orbits are the Earth departure characteristic energy, C_3, the Mars arrival v_∞, and TOF. These parameters are plotted as contour lines of constant values and allow mission designers to decide the best launch and arrival windows for interplanetary missions. Figure 5 shows an example of a porkchop plot for Earth-Mars transfers during the 2035-2036 synodic period. In order to determine the position and velocity vectors of Earth and Mars used to generate porkchop plots, 'Keplerian Elements for Approximate Position of the Major Planet' by Standish was used.[11]

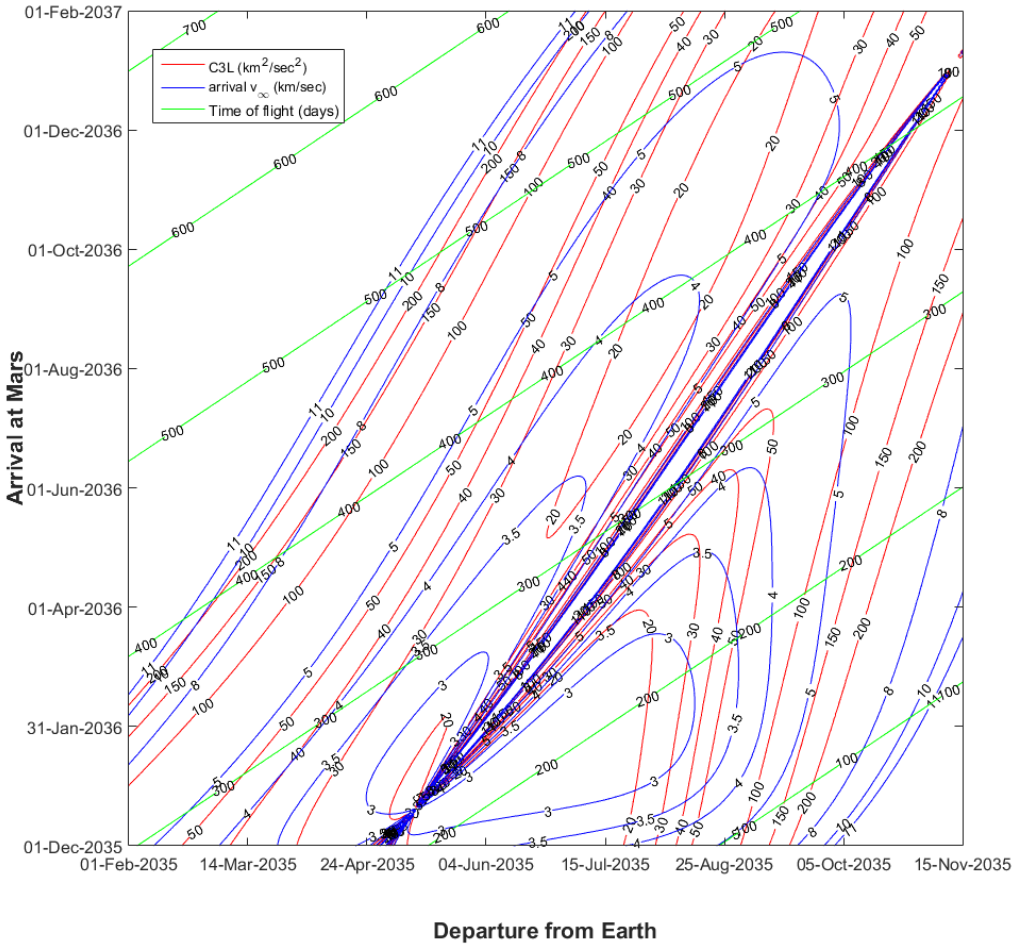

Figure 5. Porkchop plot illustrating Earth-Mars transfer for the 2035-2036 timeframe.

Figure 5 shows departure maneuvers for any dates falling within the time period that was considered (February 1, 2035 to November 15, 2035) while in reality one must take into account the geometry of the Earth and the Moon. Thus, $\vec{C_3}$ vectors were transformed from the J2000 Ecliptic (Ecl) frame to the Earth-Moon rotating reference frame. Such transformation was done by using the following Direction Cosine Matrices:[12]

- $R^{Ecl-EME}$: transforms from J2000 Ecliptic to Earth Mean Equatorial (EME) frame using the obliquity of the Earth, $\varepsilon_{\oplus} = 23.43928$ deg.
- $R^{EME-EMI}$: transforms from EME to Earth-Moon Inertial (EMI) perifocal frame using the inclination, right ascension of the ascending node, and argument of periapsis of the Moon's orbit derived from its ephemeris.
- $R^{EMI-EMR}$: transforms from EMI to Earth-Moon Rotating (EMR) reference frame using the true anomaly of the Moon's orbit derived from its ephemeris.

Consequently, $\vec{C_3}$ vectors can be converted from Ecl to EMR using the relationship:

$$\vec{C}_3^{EMR} = R^{EMI-EMR} R^{EME-EMI} R^{Ecl-EME} \vec{C}_3^{Ecl} \tag{1}$$

Using Equation (1) and the resulting $\vec{C}_3^{EMR}$, right ascension α and declination δ of departure $\vec{C_3}$ vectors can be computed. Right ascension and declination are defined in the EMR frame as shown in Figure 6.

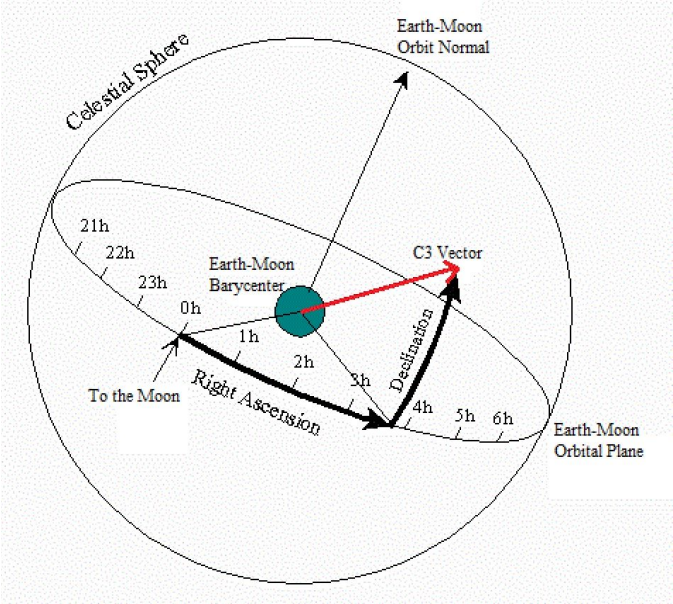

Figure 6. Geometry of Right Ascension and Declination of departure C3 vectors. Source: NOAA.[13]

$\vec{C_3}$ changes for each Earth departure date and Mars arrival date combination. Thus, from Equation (1) it is possible to calculate right ascension and declination for each $\vec{C_3}$ as a function of departure and arrival dates. Figure 7 and Figure 8 show such time-dependent relationship for right ascension and declination respectively.

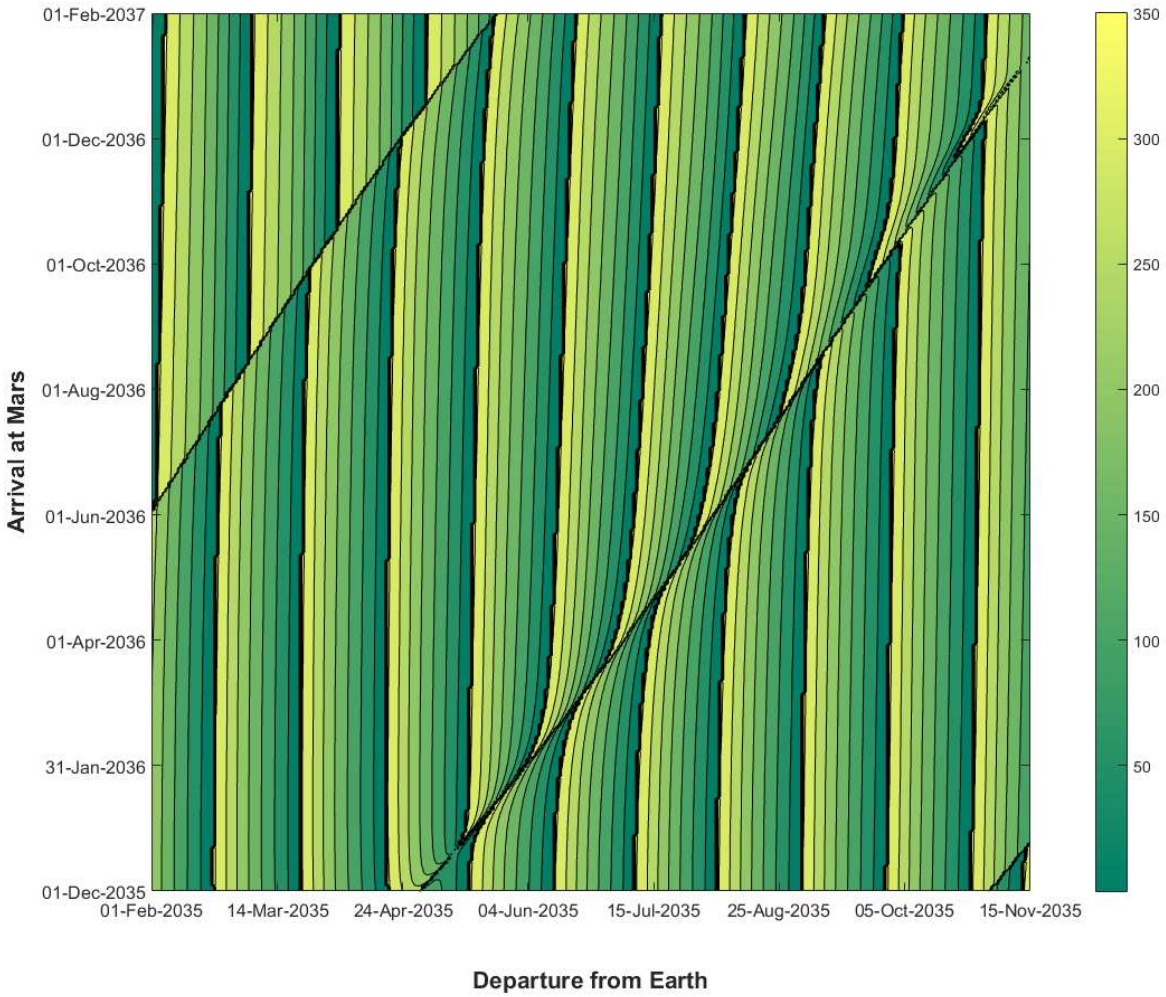

Figure 7. Right ascension (in degrees) of departure $\vec{C}_3$ vectors for the 2035-2036 Earth-Mars synodic period.

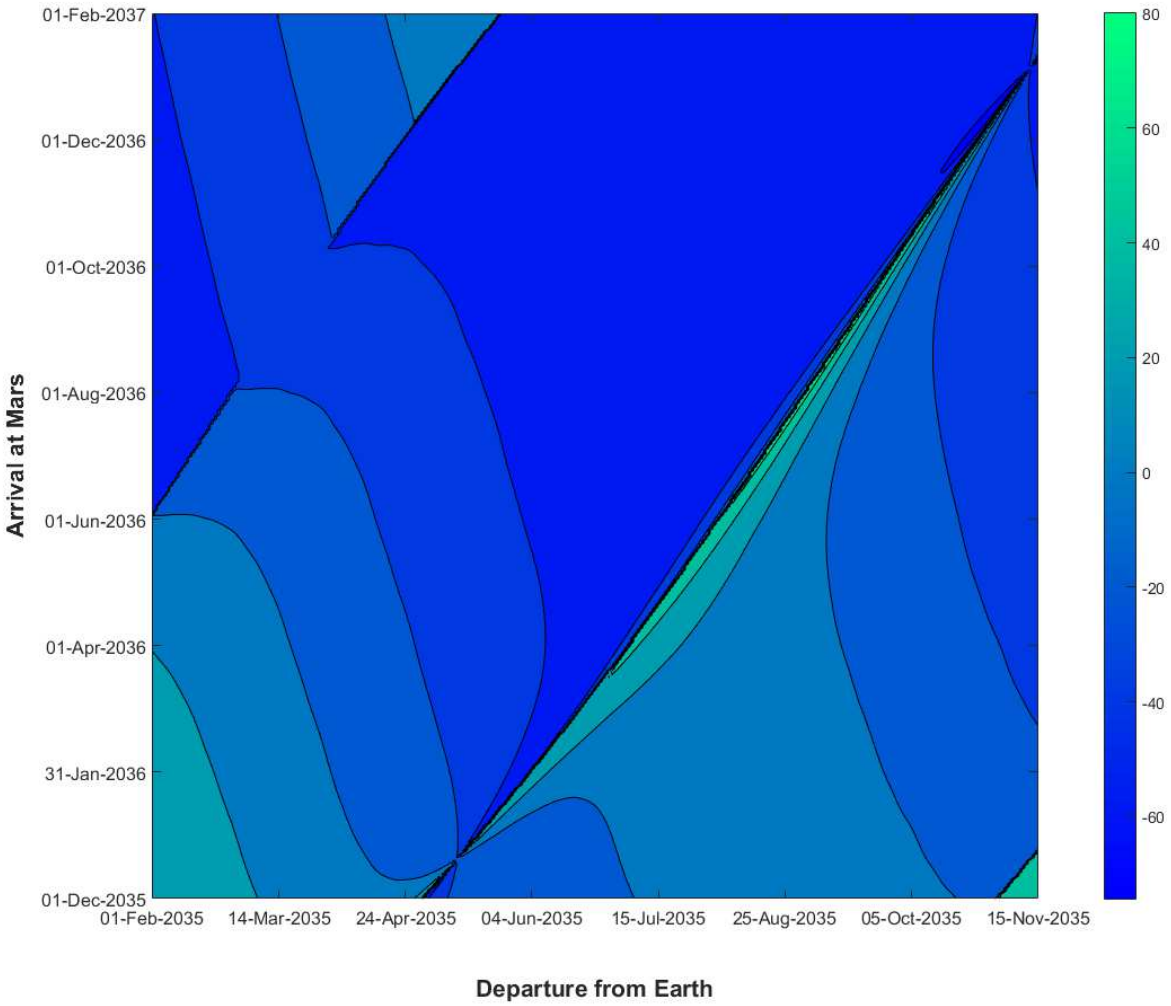

Figure 8. Declination (in degrees) of departure $\vec{C}_3$ vectors for the 2035-2036 Earth-Mars synodic period.

While right ascension varies almost uniformly from 0 to 360 degrees roughly once per month, declination is less predictable. On the other hand, right ascension is a limiting factor for Earth-Moon departures to Mars making such opportunities occur once or twice a month. Declination can significantly influence the required departure ΔV but it does not represent a limiting factor in terms of timing.

Departure ΔV was calculated by adding both DRO-Earth and Earth flyby propulsive maneuvers. An Earth flyby altitude of 300 km was chosen to avoid atmospheric drag and to maintain the spacecraft at a safe distance from the Earth's surface. Starting from a combination of departure and arrival dates, $\vec{C}_3$ magnitudes and orientation (α and δ) were determined as mentioned previously. Using the given Earth flyby altitude of 300 km and $\vec{C}_3$ magnitude, one can calculate the perigee velocity a spacecraft needs ($v_{p,n}$) in order to achieve such C_3. Right ascension α provides information on whether or not a departure trajectory exists based on the Earth-Moon geometry. Taking into account the TOF from DRO to Earth and the TOF from perigee to the Earth Sphere Of Influence (SOI), it was found that α values falling in the range of approximately 205 to 240 degrees yield feasible

trajectories two days every month.

The right ascension α of the vector $\vec{C}_3$ can be related to the right ascension θ of the spacecraft perigee in its trajectory from the DRO to the Earth (Figure 9). In Figure 9, $\gamma/2$ represents half of the turn angle due to the flyby.

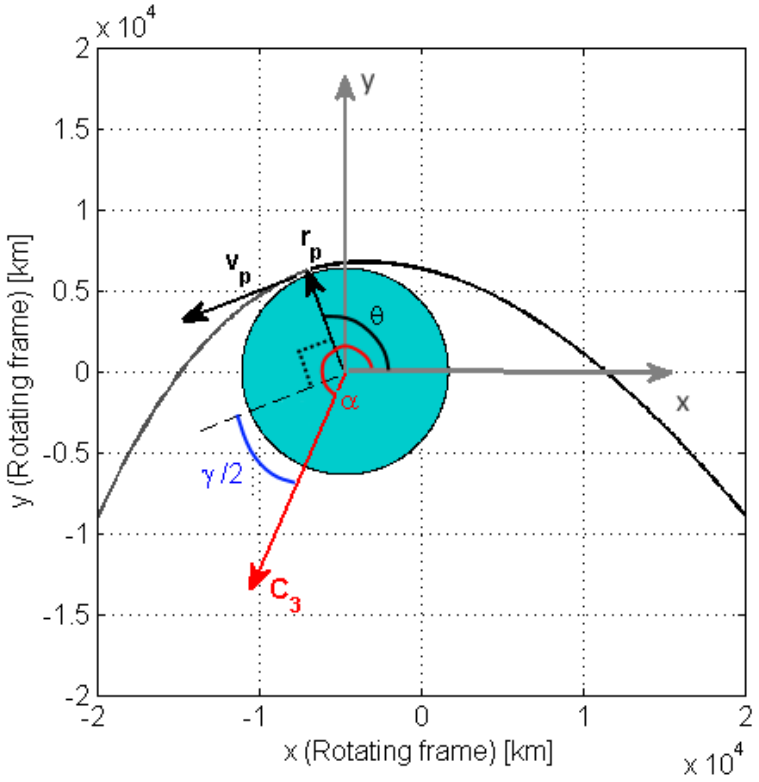

Figure 9. Geometry of the Earth flyby.

In particular, the value of θ depends on the departure point on the DRO for the DRO-Earth transfer. Different points on the DRO, all characterized by $x \geq r_{EM} + 61,500$ where r_{EM} is the Earth moon distance, were considered. A shooting method was implemented to define the departure ΔV leading to a trajectory with perigee of 300 km. The results obtained, in terms of ΔV and TOF from the DRO to the Earth perigee, are shown in Figure 10 for different departure positions on the DRO, identified by their y values. The corresponding v_p (velocity at perigee) and θ (right ascension of the perigee) values for each departure position were also computed (Figures 11).

The relationship between θ and α is (Figure 9):

$$\theta = \alpha - 90^\circ - \arcsin\left[\left(\frac{r_p}{\mu} v_{p,n}^2 - 1\right)^{-1}\right] + \frac{TOF_{hyp}}{T_{EM}}(360^\circ) \tag{2}$$

where r_p is the perigee radius of the Earth flyby, $v_{p,n}$ is the perigee velocity the spacecraft needs at r_p in order to achieve the given C_3, TOF_{hyp} is the TOF of the departure hyperbolic orbit from r_p to the Earth's SOI and T_{EM} is the Earth-Moon orbital period. Note that the term

$\arcsin\left[\left(\frac{r_p}{\mu}v_{p,n}^2 - 1\right)^{-1}\right]$ represents half of the turn angle γ obtained from the Earth flyby maneuver and the term $(TOF_{hyp})/T_{EM}(360°)$ takes into account the rotation of the Earth-Moon rotating reference frame while the spacecraft is escaping the Earth-Moon system.

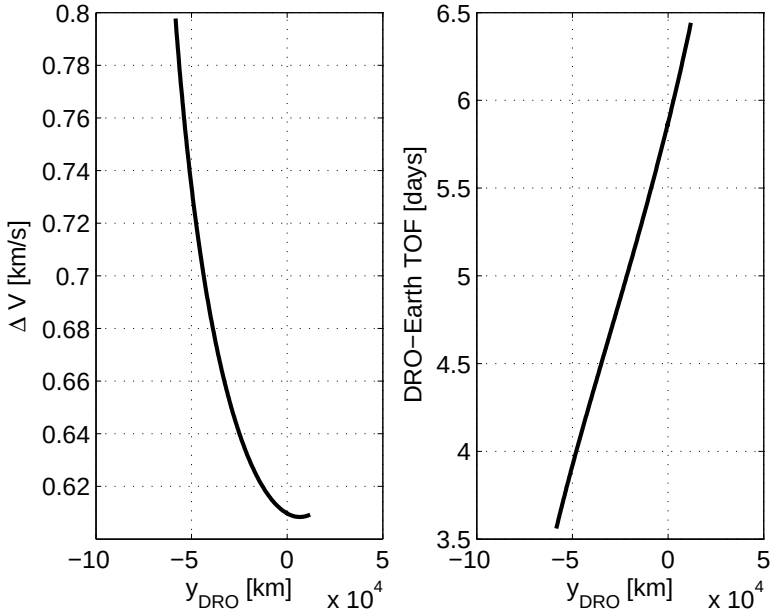

Figure 10. ΔV and TOF from a DRO as function of the departure point on the DRO.

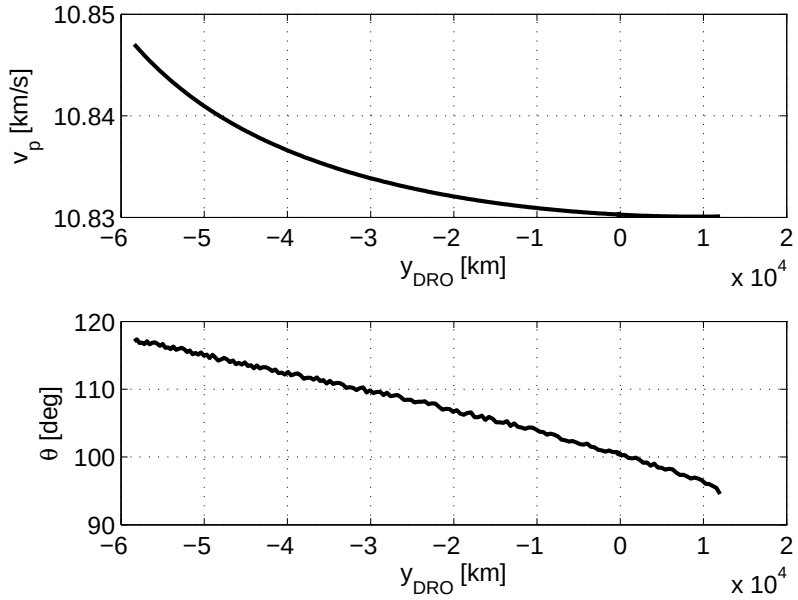

Figure 11. Velocity v_p and right ascension θ at Earth perigee, v_p.

Once $v_{p,n}$ and v_p are found, the Earth flyby ΔV, ΔV_{EF}, can be computed using the law of cosines:

$$\Delta V_{EF} = \sqrt{v_p^2 + v_{p,n}^2 - 2 v_p v_{p,n} \cos\delta} \tag{3}$$

Therefore, the departure ΔV, ΔV_{dep}, can be computed as follows:

$$\Delta V_{dep} = \Delta V_{DRO} + \Delta V_{EF} \tag{4}$$

Figure 12 shows an example of feasible departure C_3 vectors in the EMR frame.

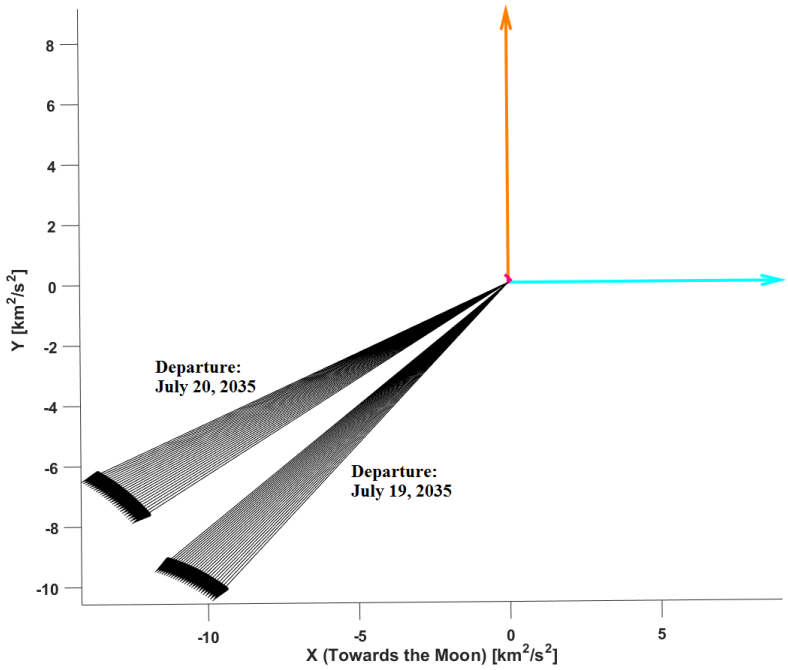

Figure 12. Example of feasible departure C_3 vectors.

Table 3 summarizes the key parameters for such departure opportunities using an Earth flyby altitude of 300 km.

Table 3. Key parameters for an example of departure opportunities.

Parameter	Minimum Value	Maximum Value
Departure Dates	July 19, 2035	July 20, 2035
Arrival Dates	January 14, 2036	February 8, 2036
C_3 at Launch [km^2/s^2]	14.683	15.8523
α [deg]	204.97	226.96
δ [deg]	9.041	10.278
Departure ΔV [km/s]	2.5783	2.8705

Figure 13 shows a sample trajectory a spacecraft would undertake to leave the DRO and reach the Earth's SOI.

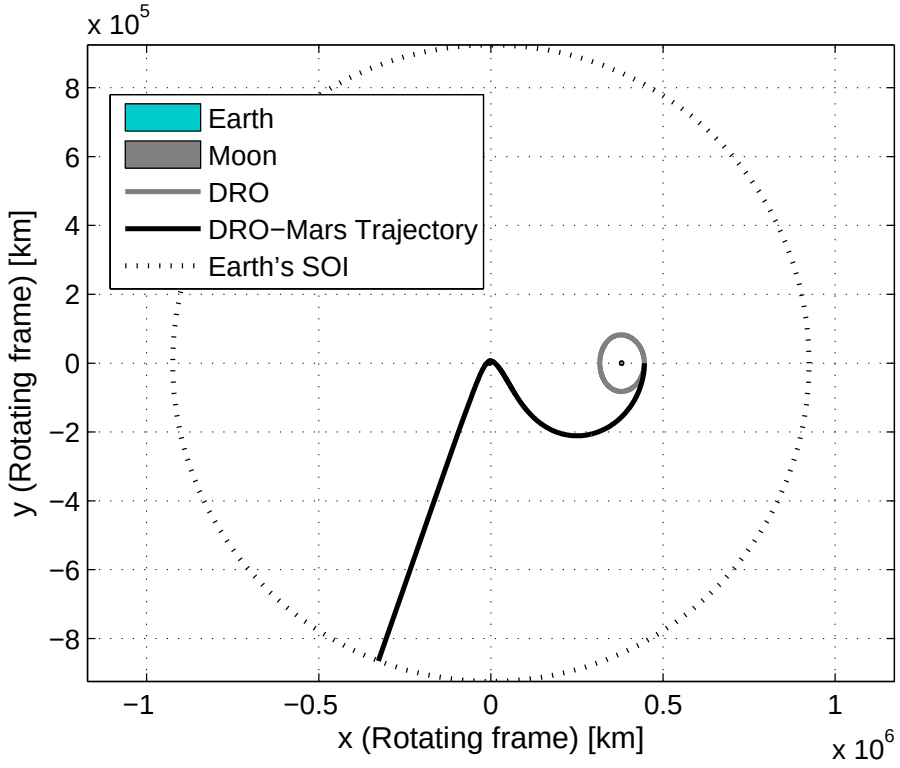

Figure 13. Total transfer.

Figure 14 and Figure 15 respectively show ΔV_{dep} and ΔV_{tot} for feasible departure trajectories during the 2035-2036 Earth-Mars synodic period. White space means that no feasible departure trajectory exists. ΔV_{tot} was calculated considering a 200x200 km altitude final Mars orbit for all cases. ΔV_{tot} does not take into account the ΔV necessary to reach the DRO from LEO; this is because a refueling depot exists in such DRO.

Table 4 summarizes the minimum ΔV_{tot} case for this synodic period and compares the key parameters with a LEO-LMO trajectory.[14]

Table 4. Minimum ΔV_{tot} case and comparison with LEO-LMO.[14]

Parameter	Value for DRO-LMO	Value for LEO-LMO
ΔV_{tot} [km/s]	3.2904	5.7582
C_3 at Launch [km^2/s^2]	10.351	10.397
v_∞ at Arrival [km/s]	2.6516	2.6283
Departure Date	June 23, 2035	June 28, 2035
Arrival Date	January 15, 2036	January 16, 2036
Time of Flight [days]	206	202

Table 5 summarizes all minimum ΔV_{tot} cases for each Earth-Mars synodic period from 2020 to 2040 and compares ΔV_{tot} and TOF with LEO-LMO trajectories.[14] Absolute lowest ΔV_{tot} for each

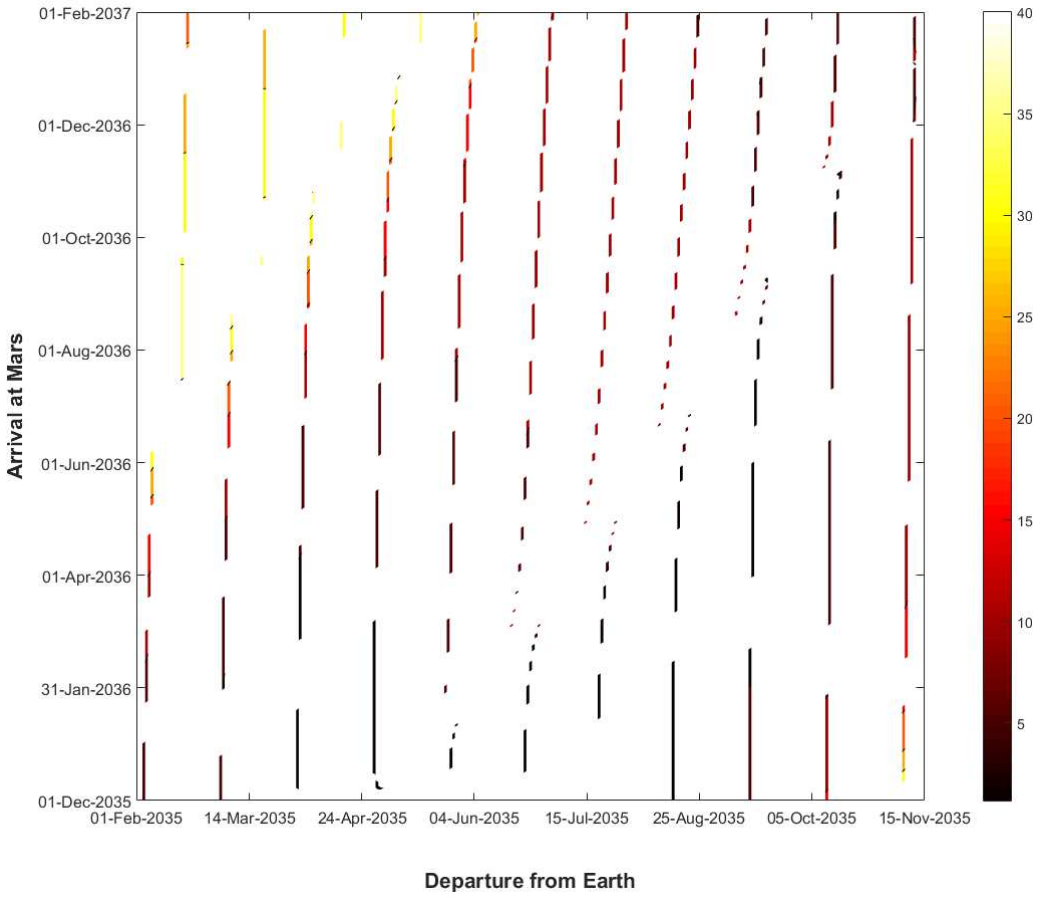

Figure 14. ΔV_{dep} **for the 2035-2036 Earth-Mars synodic period.**

trajectory type is in bold. From Table 5, it is clear that DRO-LMO maneuvers can save from 1.1 to 2.5 km/s of the ΔV_{tot}. On the other hand, departure opportunities are limited to a maximum of two days roughly every month and the use of high thrust propulsion is necessary to successfully achieve the required ΔV during the Earth flyby maneuver.

Table 5. ΔV_{tot} **and** TOF **comparison between DRO-LMO and LEO-LMO trajectories.**[14]

Synodic Period	ΔV_{tot} [km/s] DRO-LMO	TOF [days] DRO-LMO	ΔV_{tot} [km/s] LEO-LMO	TOF [days] LEO-LMO
2020-2021	3.4430	210	5.8921	207
2022-2023	3.8884	241	5.9536	347
2024-2025	3.9823	265	5.7166	333
2026-2027	4.0035	293	**5.6799**	311
2028-2029	3.5863	299	5.8722	300
2030-2031	5.0580	186	6.2268	283
2032-2033	4.0130	229	6.0583	200
2035-2036	**3.2904**	206	5.7582	202
2037-2038	3.8789	240	6.1000	348
2039-2040	4.1087	253	5.7862	340

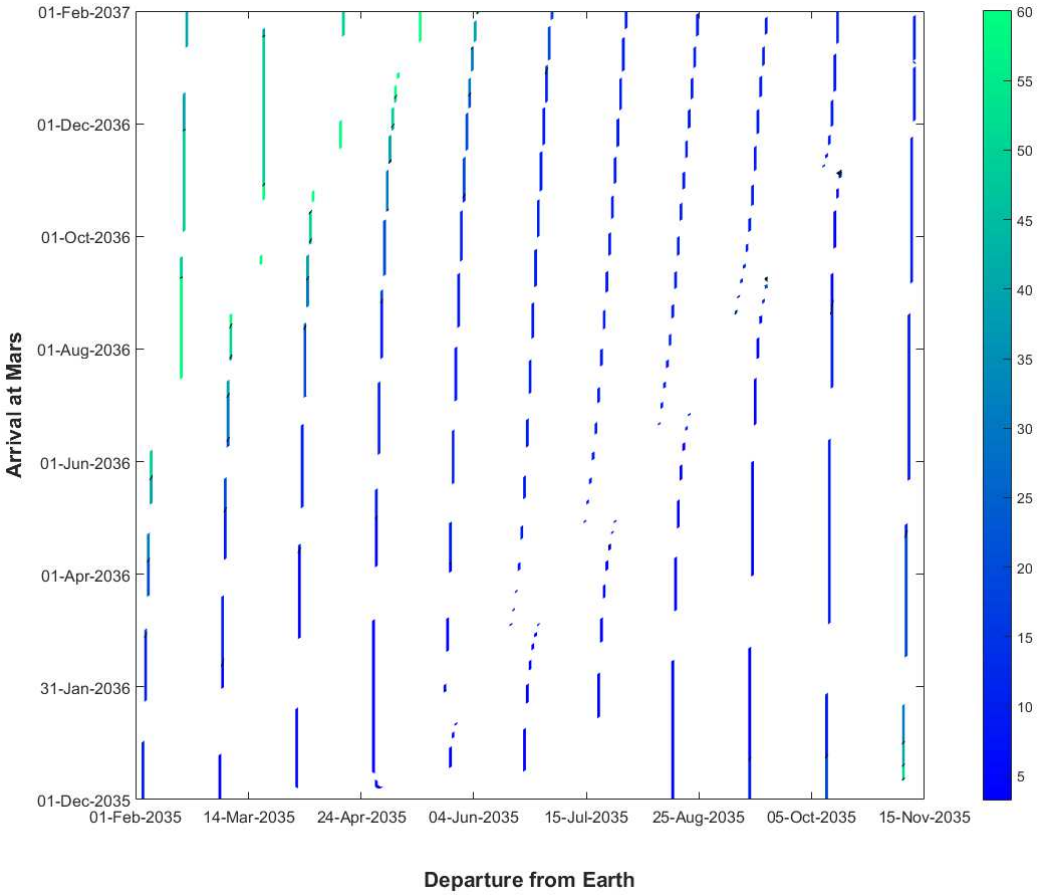

Figure 15. ΔV_{tot} for the 2035-2036 Earth-Mars synodic period.

CONCLUSION

As discussed in previous literature, a variety of Earth orbit departures such High Earth Orbits (HEO) with Low Perigee (LP) or High Perigee (HP) and cis-lunar departure orbits have been analysed. Such orbits allow spacecraft to obtain the necessary C_3 to reach destinations such as Mars and Near Earth Asteroids (NEA) of interest.[6] The analysis and results presented in this paper add a new cis-lunar departure orbit, namely from a DRO, to escape the Earth-Moon system and arrive at Mars. DRO-LMO trajectories have the advantage of needing less ΔV_{tot} than LEO-MLO trajectories. Lower ΔV_{tot} means fewer or smaller launch vehicles are needed and thus the launch cost is reduced. Additionally, the assembly of large spacecraft in a cis-lunar environment such as a DRO means that the crew would need to travel through the Van-Allen Radiation Belts two times as opposed to other HEO departure architectures.[6]

A few disadvantages of DRO-LMO trajectories exist. In fact, since the necessary ΔV to depart from the Earth-Moon system starting from a DRO is highly dependent on the position of the Moon at departure and the desired interplanetary transfer trajectory to arrive at Mars, DRO-LMO trajectories are limited to roughly once or twice every month. Additionally, since the Moons orbital elements change in time, DRO-LMO low ΔV_{tot} opportunities do not repeat as regularly as LEO-LMO low ΔV_{tot} opportunities. Conversely, because Moon DROs possess a much higher orbital energy than

LEOs, ΔV_{dep} for DRO-LMO is generally much lower than that for LEO-LMO. Additionally, even though DRO-LMO trajectories require the spacecraft to reach a DRO in the first place and hence add TOF to the total mission duration, DRO-LMO interplanetary TOFs are almost always lower than LEO-LMO interplanetary TOFs and never exceed 300 days. In this paper, only a LMO of 200x200 km altitude was considered because the focus was to decrease ΔV_{dep}. Thus, considering other Martian orbits or other orbital insertion maneuvers at Mars (e.g. aerobraking or aerocapture) can lower ΔV_{tot} even further. Another consideration is that the analysis developed to create the results presented in this paper can easily be used to develop departure DRO maneuvers to achieve other desired C_3 to target other celestial bodies.

ACKNOWLEDGMENT

Davide, Marilena and Koki would like to thank the California Institute of Technology and the Caltech Space Challenge 2015 organizers, mentors and staff members. In March 2015, they gave us the opportunity to work on and present the design of the human portion of the Asteroid Redirect Mission. This paper shows how a captured asteroid in a DRO can be used to facilitate human missions to Mars.

REFERENCES

[1] K. Ho, O. L. d. Weck, J. A. Hoffman, and R. Shishko, "Dynamic modeling and optimization for space logistics using time-expanded networks," *Acta Astronautica*, Vol. 105, No. 2, 2014, pp. 428–443.

[2] D. Arney and A. Wilhite, "Orbital propellant depots enabling lunar architectures without heavy-lift launch vehicles," *Journal of Spacecraft and Rockets*, Vol. 47, No. 2, 2010, pp. 353–360.

[3] K. Ho, K. Gerhard, A. K. Nicholas, A. J. Buck, and J. Hoffman, "On-orbit depot architectures using contingency propellant," *Acta Astronautica*, Vol. 96, 2014, pp. 217–226.

[4] C. Bezrouk and J. Parker, "Long Duration Stability of Distant Retrograde Orbits," *AIAA/AAS Astrodynamics Specialist Conference, No. AIAA*, Vol. 4424, 2014.

[5] G. L. Condon and J. Williams, "Asteroid Redirect Crewed Mission Nominal Design and Performance," *SpaceOps 2014 Conference*, 5-9 May 2014, Pasadena, CA.

[6] R. G. Merrill, D. Komar, M. Qu, J. Chrone, N. Strange, and D. Landau, "An initial comparison of selected Earth departure options for solar electric propulsion missions," *Aerospace Conference, 2012 IEEE*, IEEE, 2012, pp. 1–18.

[7] B. G. Drake, S. J. Hoffman, and D. W. Beaty, "Human exploration of Mars, design reference architecture 5.0," *Aerospace Conference, 2010 IEEE*, IEEE, 2010, pp. 1–24.

[8] M. Landgraf, M. Düring, and F. Renk, "Mission Design Aspect of European Elements in the International Space Exploration Framework," *Journal of Guidance Control and Dynamics*, Vol. 30, No. 5, 2007, p. 1261.

[9] V. Boccia, D. Conte, S. Dandavino, P. Das, T. d. Roche, M. Di Carlo, D. Fries, R. Goel, K. Ho, H. Jethani, M. Khatsenko, M. Lapotre, A. Morita, B. Tandy, and L. Wilson, *L-DORADO: Lunar reDirected Orbiting Resource Asteroid Demonstration and Operation*. Presented at the California Institute of Technology Space Challenge in March 2015.

[10] L. Capdevila, D. Guzzetti, and K. Howell, "Various Transfer Options from Earth into Distant Retrograde Orbits in the Vicinity of the Moon," *AAS/AIAA Space Flight Mechanics Meeting*, 2014, pp. AAS14–467.

[11] E. M. Standish, "Keplerian elements for approximate positions of the major planets," *available from the JPL Solar System Dynamics web site (http://ssd. jpl. nasa. gov/)*, 2006, accessed 1 June, 2015.

[12] D. A. Vallado and W. D. McClain, *Fundamentals of astrodynamics and applications*. Springer Science & Business Media, 2001.

[13] E. W. Team *et al.*, "ESRL Global Monitoring Division-GRAD Group," http://www.esrl.noaa.gov/gmd/grad/solcalc/celsphere.gif.

[14] D. Conte, "Determination of Optimal Earth-Mars Trajectories to Target the Moons of Mars," Master's thesis, The Pennsylvania State University, 2014.